Protonation of *trans*-$[Mo(C_2H_4)_2(Ph_2PCH_2CH_2PPh_2)_2]$: Sites of Protonation and Factors influencing the Formation of Ethane and Ethylene

Kay E. Oglieve and Richard A. Henderson*
AFRC Institute of Plant Science Research, Nitrogen Fixation Laboratory, University of Sussex, Brighton BN1 9RQ, UK

The mechanism of the formation of ethane and ethylene in the reactions of *trans*-$[Mo(C_2H_4)_2(dppe)_2]$ (dppe = $Ph_2PCH_2CH_2PPh_2$) with HX (X = Cl or Br) in tetrahydrofuran at 25.0 °C has been established by a combination of stopped-flow spectrophotometry, detailed product analysis and kinetic investigation of the evolution of hydrocarbons, together with characterisation of the key intermediates by multinuclear NMR spectroscopy. Addition of anhydrous HX to *trans*-$[Mo(C_2H_4)_2(dppe)_2]$ rapidly generates $[MoH(C_2H_4)(dppe)_2]^+$ by two pathways: direct protonation at the metal or protonation at the ethylene ligand to form $[Mo(C_2H_5)(C_2H_4)(dppe)_2]^+$ followed by migration of a β-hydrogen atom from the ethyl ligand to the metal. This migration step is reversible and at low concentrations of HCl $[Mo(C_2H_5)(C_2H_4)(dppe)_2]^+$ slowly loses ethylene. Subsequent binding of chloride ultimately results in the formation of ethane, and *trans*-$[MoCl_2(dppe)_2]$. At higher concentrations of HCl further protonation of $[MoH(C_2H_4)_2(dppe)_2]^+$ occurs and $[MoH_2(C_2H_4)_2(dppe)_2]^{2+}$ is the dominant solution species which loses both ethylene ligands to form $[MoH_2Cl_2(dppe)_2]$. Quantitative analysis of the hydrocarbon product distribution at various concentrations of HCl confirms the nature of these pathways under an atmosphere of dinitrogen or argon. In the presence of carbon monoxide or dihydrogen the hydrocarbon product distribution is different. The relevance of these studies to the understanding of the different substrate specificities of the molybdenum- and vanadium-based nitrogenases is discussed, as are the factors influencing the rates of protonation of the metal in $[ML_2(dppe)_2]$ (M = Mo or W; L = N_2, C_2H_4 or 2 H).

Although it has been known for some time that protonation of simple alkene complexes can occur at the metal or the co-ordinated alkene,[1] it is only recently that the relative rates of protonation at these two sites has been defined, at least for *trans*-$[W(C_2H_4)_2(dppe)_2]$ (dppe = $Ph_2PCH_2CH_2PPh_2$).[2] Here we report studies on *trans*-$[Mo(C_2H_4)_2(dppe)_2]$ which complement this work, but, more important, define the pathways by which ethane or ethylene is released from the system (Scheme 1). Our interest in the factors which discriminate between ethane formation and ethylene evolution arose from the various substrate specificities of the nitrogenases. It has been known for some time that under an atmosphere of acetylene the molybdenum-based nitrogenase reduces acetylene to ethylene,[3] and this reaction has been used widely in studies on biological nitrogen fixation. However, under identical conditions the vanadium-based enzyme produces some ethane (*ca.* 3% of the electron flux)[4] and, under an atmosphere of ethylene, the molybdenum-based nitrogenase also gives some ethane (< 1% of the electron flux).[5] The results described in this paper lead to a rationalisation of this substrate specificity for the two enzymes.

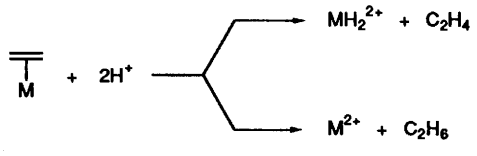

Scheme 1

Results

The reactions of *trans*-$[Mo(C_2H_4)_2(dppe)_2]$ with HX (X = Cl or Br) in tetrahydrofuran (thf) at 25.0 °C to produce ethane and/or ethylene fall into two distinct stages: the initial protonation reactions of the parent complex, and the slow release of the hydrocarbons. We shall present the results for the two stages in separate sections.

Rapid Protonation of trans-$[Mo(C_2H_4)_2(dppe)_2]$.—Upon mixing a thf solution of *trans*-$[Mo(C_2H_4)_2(dppe)_2]$ with a solution of anhydrous HX in a stopped-flow apparatus at 25.0 °C absorbance changes typified by those at λ = 400 nm shown in Fig. 1 are observed. The sequence of events is as follows. (*i*) An initial rapid absorbance change, complete within the dead-time of the stopped-flow apparatus (2 ms). The absorbance of unreacted *trans*-$[Mo(C_2H_4)_2(dppe)_2]$ is shown in this figure at A = 0.43. (*ii*) In the second phase a decreasing exponential trace is observed (complete within *ca.* 1 s in Fig. 1), and, finally, (*iii*) a relatively slow exponential increase over the next *ca.* 14 s. the kinetic data for all three phases with both HCl and HBr are shown in Table 1.

Our interpretation of the chemistry associated with each of these phases is shown on the periphery of the trace in Fig. 1, and is based [at least for phases (*i*) and (*ii*)] on similar behaviour in the reactions of *trans*-$[W(C_2H_4)_2(dppe)_2]$ with HX.[2] The tungsten system results ultimately in the protonation of the metal as shown in equation (1). However, the molybdenum

$$trans\text{-}[W(C_2H_4)_2(dppe)_2] + HX \longrightarrow [WH(C_2H_4)_2(dppe)_2]X \quad (1)$$

system is more complicated, and involves the loss of hydrocarbons. Analysis of the magnitude of the initial absorbance change in phase (*i*) of the reactions with *trans*-$[Mo(C_2H_4)_2(dppe)_2]$ as a function of the acid concentration demonstrates that this step corresponds to a single protonation of the

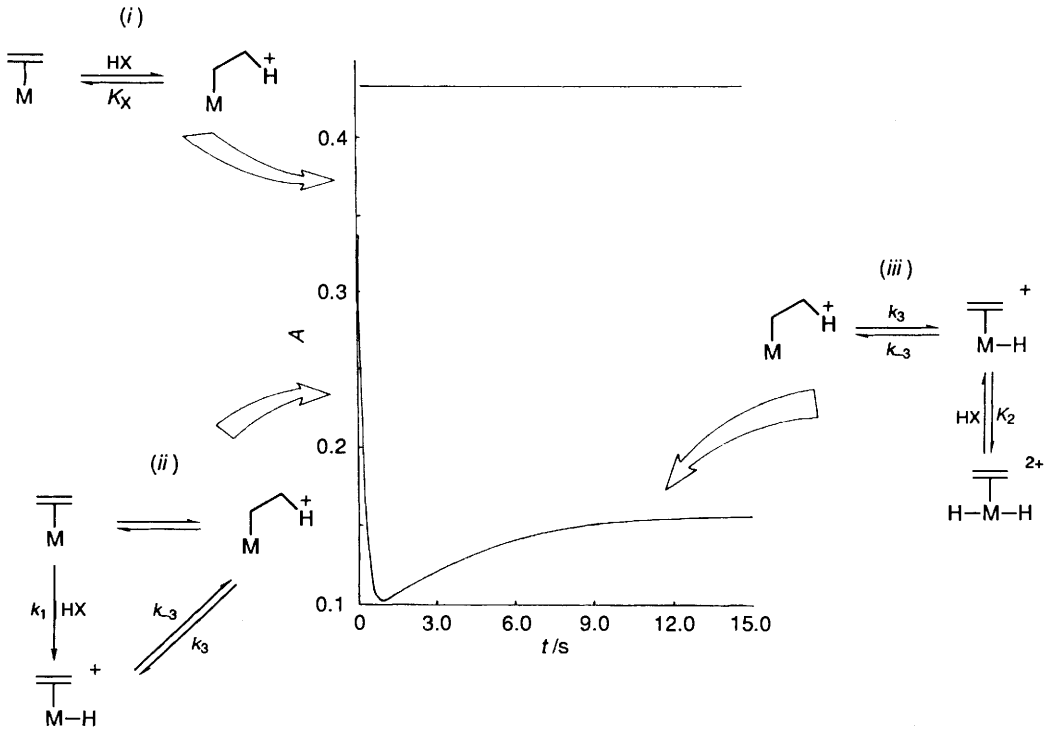

Fig. 1 Typical absorbance–time trace for the reaction of *trans*-$[Mo(C_2H_4)_2(dppe)_2]$ ([Mo] = 8.6 × 10^{-5} mol dm^{-3}) with HCl (10.0 mmol dm^{-3}) in thf at 25.0 °C, λ = 400 nm

molybdenum complex as shown in Fig. 2 (insert) with K_{Cl} = 18.0 ± 0.2 dm^3 mol^{-1} or K_{Br} = (7.0 ± 0.8 × 10^2 dm^3 mol^{-1} where K_{Cl} and K_{Br} are the equilibrium constants for protonation of the ethylene ligand by HCl or HBr respectively. The details of this analysis are given in the legend to Fig. 2. The subsequent absorbance decay [phase (*ii*)] exhibits a first-order dependence on the concentration of molybdenum complex and a dependence on the concentration of HX as described by equation (2), and shown in Fig. 2, where here and throughout

$$k_{obs} = a + b[HX] \quad (2)$$

this paper k_{obs} is the pseudo-first-order rate constant determined in the presence of an excess of acid. When X = Cl, a = 0.22 ± 0.01 s^{-1}, b = (4.60 ± 0.1) × 10^2 dm^3 mol^{-1} s^{-1}, k_H/k_D = 1.64 and when X = Br, b = (1.0 ± 0.1) × 10^5 dm^3 mol^{-1} s^{-1}. The rapidity of the reaction with HBr precludes an accurate determination of the value of a in this case. This same problem was encountered in the studies with *trans*-$[W(C_2H_4)_2(dppe)_2]$ and HBr.[2]

By analogy with the studies on *trans*-$[W(C_2H_4)_2(dppe)_2]$, the two phases (*i*) and (*ii*) for the reaction of HX with *trans*-$[Mo(C_2H_4)_2(dppe)_2]$ correspond to the formation of $[MoH(C_2H_4)_2(dppe)_2]^+$ by the two pathways shown on the left-hand side of Fig. 1, the intimate details of which we shall discuss later. However, in contrast to the tungsten species the molybdenum system undergoes rapid intramolecular rearrangement which results in the rapid equilibration of the hydrido-species and the ethyl complex, *trans*-$[Mo(C_2H_5)(C_2H_4)(dppe)_2]^+$. This is confirmed by isolation and characterisation of this intermediate by ^1H and ^{31}P NMR spectroscopy both in this study (see Table 2) and in earlier work.[1] In particular the ^{31}P-{^1H} NMR spectrum at 25.0 °C is deceptively simple, consisting of a pair of doublets both with J(PP) = 81.8 Hz and consistent with the AA′BB′ pattern reported earlier for this and analogous complexes.[1,6,7] This spectral pattern is a consequence of a basic pentagonal-bipyramidal structure with two phosphorus atoms in the axial positions, which undergoes rapid exchange involving the migration of the hydride onto one of the ethylene ligands followed by an in-place rotation of the derived ethyl species. We have also shown by ^{31}P-{^1H} NMR spectroscopy that in solution the same intermediate is formed both with HCl and low concentrations of HBr, and in addition that the visible absorption spectrum of the isolated material is identical to that of the intermediate formed at the end of phase (*ii*) as shown in Fig. 3. From hereon we shall refer to this isolated material as $[MoH(C_2H_4)_2(dppe)_2][HBr_2]$, but with due regard to the observations that in solution this structural integrity is not retained.

We have not been successful in investigating the variable-temperature NMR spectra of $[MoH(C_2H_4)_2(dppe)_2]^+$ because of the poor solubility of this complex, and because the ensuing release of hydrocarbons complicates the interpretation. Proton-undecoupling experiments using ^{31}P NMR spectroscopy only resulted in broadened signals.

The final phase observed on the stopped-flow time-scale [phase (*iii*)] exhibits different kinetics with HCl to those observed with HBr. With HBr, there is a first-order dependence on the concentration of molybdenum complex and inhibition by an increasing concentration of acid. Graphical analysis of the data as shown in Fig. 4 results in the rate equation (3). In

$$k_{obs} = (0.25 \pm 0.02)/\{1 + (1.77 \pm 0.30) \times 10^3 [HBr]\} \quad (3)$$

contrast, with HCl phase (*iii*) exhibits a dependence on the concentration of acid in accord with equation (2), with a = 0.22 ± 0.02 s^{-1} and b = 14.0 ± 0.5 dm^3 mol^{-1} s^{-1}.

This third phase, which is not observed in the tungsten system, involves further protonation of $[MoH(C_2H_4)_2(dppe)_2]^+$ to give $[MoH_2(C_2H_4)_2(dppe)_2]^{2+}$. We have not been able to isolate this material, all attempts resulting in the isolation of salts of the monocation, presumably because of the rapid equilibration between these two species and the poorer solubility of $[MoH(C_2H_4)_2(dppe)_2]^+$ salts. However, in thf the ^{31}P-{^1H} NMR spectrum of $[MoH_2(C_2H_4)_2(dppe)_2]^{2+}$ has been measured (Table 2) when [HBr] = 10 mmol dm^{-3}, where the dication is the dominant species (>95% of total molybdenum present). The spectrum is very similar to that of [MoH-

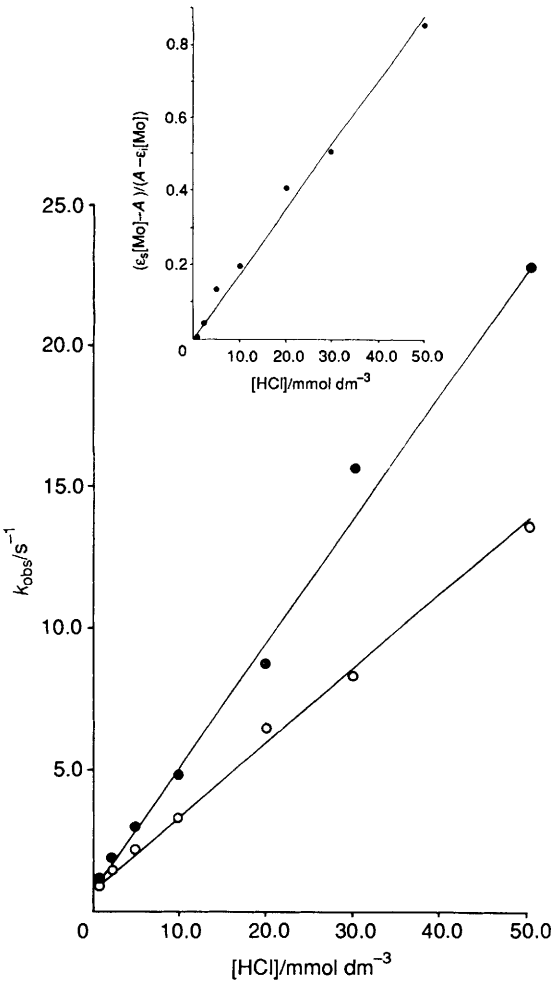

Fig. 2 Plot (insert) of $(\varepsilon_s[Mo] - A)/(A - \varepsilon_i[Mo])$ against the concentration of HCl at 25.0 °C in thf, where A = initial absorbance (after 2 ms) determined at the particular acid concentration, and allowing for any absorbance 'lost' in the more rapid reactions by calculating the initial absorbance of phase (*ii*) using the values of k_{obs} for this phase at the particular acid concentration being studied; [Mo] = concentration of $[Mo(C_2H_4)_2(dppe)_2]$ (1×10^{-4} mol dm^{-3}), ε_s = absorption coefficient of $[Mo(C_2H_4)_2(dppe)_2]$ (5.0×10^3 dm^3 mol^{-1} cm^{-1}), and ε_i = absorption coefficient of ethyl complex (2.6×10^3 dm^3 mol^{-1} cm^{-1}) at λ = 400 nm determined from the maximum absorbance jump measured in the studies with HBr. The main Figure shows the dependence of k_{obs} on the acid concentration for the reaction of *trans*-$[Mo(C_2H_4)_2(dppe)_2]$ with HCl (●) or ^{2}HCl (○) in thf at 25.0 °C

$(C_2H_4)_2(dppe)_2]^+$ being a pair of doublets, both with J(PP) = 73.5 Hz, consistent with an AA'BB' pattern. It is consistent with the basic structure shown in Scheme 2, but again involving rapid intramolecular migration processes associated with the hydride and ethylene ligands, analogous to those of $[MoH(C_2H_4)_2(dppe)_2]^+$. Thus if we consider the addition of the first proton to *trans*-$[Mo(C_2H_4)_2(dppe)_2]$ as occurring on one side of the diphosphine plane to give $[MoH(C_2H_4)_2(dppe)_2]^+$, the addition of the second proton occurs on the other side of the phosphine plane.

The decrease in the value of J(PP) between $[MoH(C_2H_4)_2(dppe)_2]^+$ and $[MoH_2(C_2H_4)_2(dppe)_2]^{2+}$ is consistent with increased protonation of the metal, and a similar effect has been observed in the values of J(PH) for $[OsH_4\{P(C_6H_4Me\text{-}p)_3\}_3]$ [J(PH) = 9 Hz] and $[OsH_5\{P(C_6H_4Me\text{-}p)_3\}_3]^+$ [J(PH) = 4 Hz].[8]

The species $[MoH_2(C_2H_4)_2(dppe)_2]^{2+}$ is a further member of the series $[MoH_2L_2(dppe)_2]^{n+}$ (L = Cl,[9] Br, MeCN,[10,11] C_2H_4 or PhS[12]).

The kinetics of phases (*i*)–(*iii*) are unchanged in the presence of carbon monoxide or ethylene.

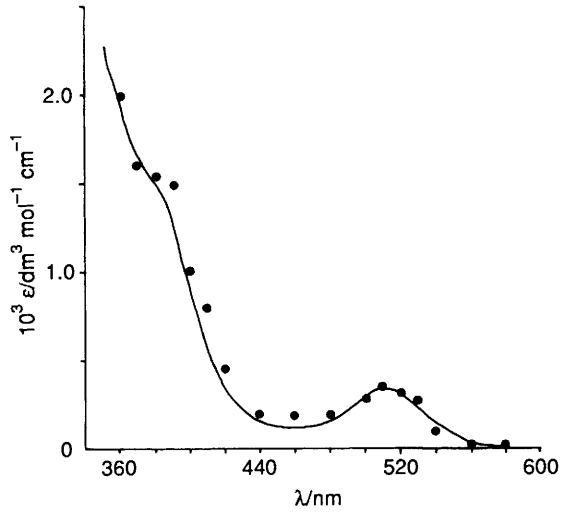

Fig. 3 Visible absorption spectrum of $[MoH(C_2H_4)_2(dppe)_2]Br$ in thf (solid curve), and the spectrum of the intermediate formed at the end of phase (*ii*) (●) measured on the stopped-flow spectrophotometer

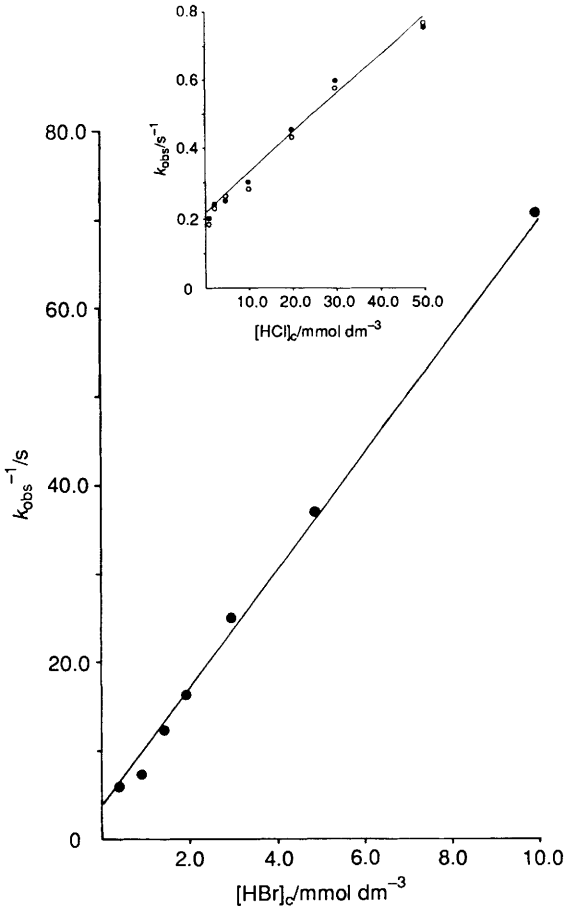

Fig. 4 Dependence (insert) of k_{obs} on the concentration of HCl (●) or ^{2}HCl (○) for phase (*iii*) in the reaction of *trans*-$[Mo(C_2H_4)_2(dppe)_2]$ with HCl in thf at 25.0 °C; $[HCl]_c$ = [HCl] − [Mo], to allow for consumption of 1 mole equivalent of acid in phases (*i*) and (*ii*). The main figure shows a plot of $1/k_{obs}$ against the concentration of HBr in the reaction of *trans*-$[Mo(C_2H_4)_2(dppe)_2]$ with HBr in thf at 25.0 °C; $[HBr]_c$ = [HBr] − [Mo]

Formation of Hydrocarbons.—The slow evolution of both ethane and ethylene was monitored by sampling the gaseous atmosphere above the reaction mixture. The kinetics for the formation of the hydrocarbons exhibits a first-order dependence on the concentration of molybdenum complex, but independent

Table 1 Kinetic data for all phases of the reactions between *trans*-$[Mo(C_2H_4)_2(dppe)_2]$ and HX (X = Cl or Br) in thf at 25.0 °C. Stopped-flow studies were performed at λ = 400 nm

X	[HX]/ mmol dm^3	A^a (*i*)	k_{obs}/s^{-1} (*ii*)	(*iii*)	C_2H_6	C_2H_4
Cl[b]	1.0	0.50	1.10	0.20		
	2.5	0.49	1.96	0.24		
	5.0	0.47	2.97	0.25		
	10.0	0.46	4.80	0.30		
	20.0	0.43	8.69	0.45		
	30.0	0.42	15.90	0.60		
	50.0	0.39	22.90	0.75		
Cl[c]	2.5	0.49	1.65	0.20		
	5.0	0.48	3.00	0.23		
	20.0	0.44	8.80	0.42		
Cl[d]	20.0				3.1×10^{-4}	3.1×10^{-4}
	50.0				3.3×10^{-4}	3.1×10^{-4}
	90.0				3.3×10^{-4}	2.9×10^{-4}
Cl[e]	50.0					3.3×10^{-4}
	90.0					3.1×10^{-4}
Cl[f]	1.0	0.50	0.93	0.18		
	2.5	0.48	1.50	0.23		
	5.0	0.48	2.20	0.26		
	10.0	0.47	3.31	0.29		
	20.0	0.44	6.45	0.43		
	30.0	0.42	8.16	0.57		
	50.0	0.39	13.6	0.76		
Br	0.5	0.44	36.2	0.17		
	1.0	0.40	103.2	0.13		
	1.5	0.38	181.7	0.085		
	2.0	0.35	223.9	0.063		
	3.0	0.34	338.0	0.040		
	5.0	0.31	450.0	0.027		
	10.0		too fast	0.015		

[a] Calculated initial absorbance, extrapolating exponential of phase (*ii*) to $t = 0$. [b] [Mo] = 0.05–2.0 mmol dm^{-3}; k_{obs} for all phases invariable in this concentration range. [c] Studies under an atmosphere of C_2H_4; identical results obtained under an atmosphere of H_2 or CO. [d] Kinetic studies for the formation of the hydrocarbons under N_2. [e] Kinetic studies for the formation of the hydrocarbons under CO. [f] Studies using ^{2}HCl generated from $SiMe_3Cl$ and MeO^2H.

Table 2 Analytical and spectroscopic characterisation of complexes

Complex	Analysis[a] (%) C	H	IR/cm^{-1}	NMR (δ) ^{1}H[b]	^{31}P[c]
$[Mo(C_2H_4)_2(dppe)_2]$	70.9 (70.9)	6.2 (5.9)		0.10 (4, br, H_2CCH_2) 0.39 (4, br, H_2CCH_2)	−78.0 (s)
$[MoH(C_2H_4)_2(dppe)_2][HBr_2]$	59.9 (60.5)	4.8 (5.2)			−80.0 (d), −92.2 (d), *J*(PP) = 81.8 (AA′BB′ pattern)
$[MoH_2(C_2H_4)_2(dppe)_2]^{2+}$	*d*				−76.2 (d), −92.2 (d), *J*(PP) = 73.5 (AA′BB′ pattern)
$[MoH_2Cl_2(dppe)_2]$	64.4 (64.6)	5.1 (5.2)	1880w [ν(Mo–H)]	−4.6 (2) [q, *J*(PH) = 45, Mo-H]	−70.8 (t), −97.5 (t), *J*(PP) = 10.2
$[MoH_2Br_2(dppe)_2]$	58.6 (59.0)	4.6 (4.7)	1940w [ν(Mo–H)]	−5.6 (2) [q, *J*(PH) = 54, Mo–H]	−74.6 (t), −100.0 (t), *J*(PP) = 10.2
$[MoCl_2(dppe)_2]$	64.5 (64.7)	5.2 (5.0)	320m [ν(Mo–Cl)]		

[a] Calculated values shown in parentheses. [b] Chemical shifts referenced to $SiMe_4$, *J* in Hz; spectra recorded in [$^2H_8$]tetrahydrofuran. All spectra show signals at δ 2.8–3.0 (8, br, CH_2CH_2) and 7.0–7.6 (40, m, Ph). [c] Chemical shifts referenced to $P(OMe)_3$, spectra recorded in thf or CH_2Cl_2. [d] Not isolated, detected in solution, see text.

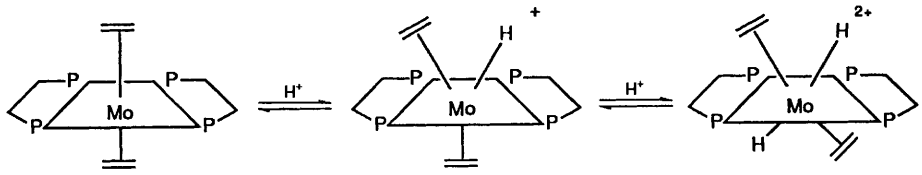

Scheme 2

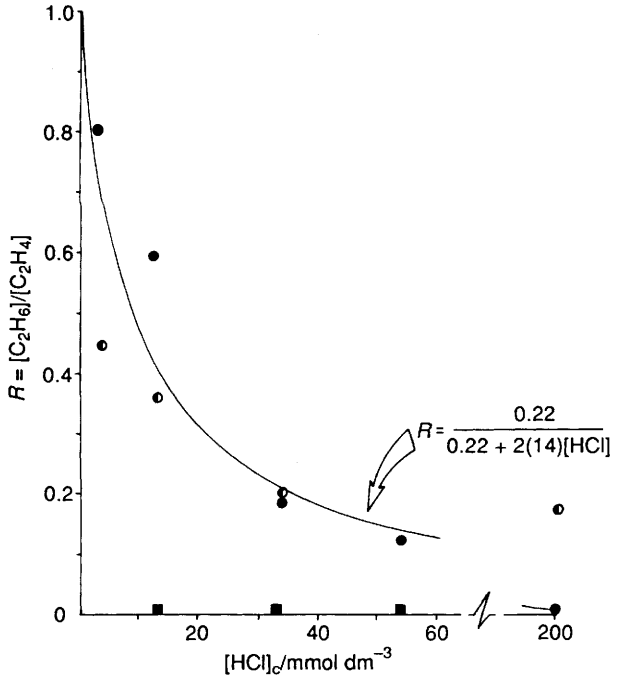

Fig. 5 Dependence of the hydrocarbon product ratio, $R = [C_2H_6]/[C_2H_4]$, in the reaction of *trans*-$[Mo(C_2H_4)_2(dppe)_2]$ with HCl in thf at 25.0 °C. The concentration of HCl has been corrected, $[HCl]_c = [HCl] - [Mo]$, to allow for the rapid consumption of 1 mole equivalent of acid to form $[MoH(C_2H_4)_2(dppe)_2]^+$ prior to the release of hydrocarbons; R was determined under an atmosphere of dinitrogen or argon (●), under an atmosphere of dihydrogen (◐), or under an atmosphere of carbon monoxide (■)

of the concentration of the acid, and independent of whether the reaction is under an atmosphere of dinitrogen, argon or carbon monoxide, with a rate constant $k_{obs} = (3.1 \pm 0.2) \times 10^{-4}$ s^{-1}.

The hydrocarbon product distribution depends both on the concentration of HCl and on the nature of the reaction atmosphere. Thus, under argon or dinitrogen at low concentrations of HCl the hydrocarbon product ratio $R = [C_2H_6]/[C_2H_4]$ from *trans*-$[Mo(C_2H_4)_2(dppe)_2]$ approaches 1.0:1 as shown in Fig. 5. However, as the concentration of HCl is increased the proportion of ethane decreases such that, at [HCl] = 200 mmol dm^{-3}, ethylene is the exclusive product, $R = 0$. At all acid concentrations the total amount of hydrocarbon detected was better than 85% of that expected for the release of both hydrocarbon fragments from *trans*-$[Mo(C_2H_4)_2(dppe)_2]$.

The molybdenum products formed at low and high acid concentrations have been isolated and identified. At low acid concentrations ([HCl]/[Mo] = 2.0:1) the product is *trans*-$[MoCl_2(dppe)_2]$, identified by elemental analysis and comparison of its IR and FIR spectra with an authentic sample of the dichloride (Table 2). Further spectroscopic characterisation of this material is precluded since it is both NMR and EPR 'silent'. At high concentrations of acid, under conditions where ethylene is the exclusive hydrocarbon product, the molybdenum product is $[MoH_2X_2(dppe)_2]$ (Table 2). In particular the characteristic ^{31}P-$\{^1H\}$ NMR spectra of these species allowed easy identification in solution. For spectroscopic comparison authentic samples of $[MoH_2X_2(dppe)_2]$ were prepared by the reaction of $[MoH_4(dppe)_2]$ with anhydrous HX in thf.[11]

Under an atmosphere of carbon monoxide ethylene is the only hydrocarbon product formed at all concentrations of HCl as shown in Fig. 5. Under an atmosphere of dihydrogen the product distribution ratio R does not vary much over the range [HCl] = 0–200 mmol dm^{-3}, but it does tend towards 0.50 and 0.15 at low and high acid concentration respectively.

Discussion

This study on the formation of ethane and evolution of ethylene by protonation of *trans*-$[Mo(C_2H_4)_2(dppe)_2]$ in thf is a rare example of a multistep mechanism being defined in detail. This is possible because the four major steps of the reaction (three on the stopped-flow time-scale involving the formation of the 'precursor complexes' which subsequently release the hydrocarbons, and the fourth, on a more conventional time-scale, involving the release of ethane and ethylene) are clearly separated from one another. All of the kinetic and product analysis results presented above are consistent with the mechanism shown in Scheme 3. In general terms, the important feature about this mechanism is that all of the species represented have been isolated, or detected in solution, and characterised. The elementary rate and equilibrium constants are summarised in Table 3, together with the comparable values observed in the analogous but simpler tungsten system.[2]

Formation of Precursor Complexes.—Upon mixing solutions of anhydrous HX and *trans*-$[Mo(C_2H_4)_2(dppe)_2]$ the initial reaction, complete within the dead-time of the stopped-flow apparatus ($k_x > 1 \times 10^6$ dm^3 mol^{-1} s^{-1}), is the protonation of the ethylene ligand to give the corresponding ethyl species. Inspection of the values of the equilibrium constants, K_x for this step shown in Table 3 reveals that an ethylene co-ordinated to molybdenum has a greater affinity for a proton than when bound to tungsten. This behaviour contrasts with that observed for nitrogen ligands such as dinitrogen and nitride at the 'M(dppe)$_2$' core, where tungsten renders the nitrogen ligand more basic than does molybdenum.[13]

The initial protonation of the parent complex results in an equilibrium mixture of *trans*-$[Mo(C_2H_4)_2(dppe)_2]$ and $[Mo(C_2H_5)(C_2H_4)(dppe)_2]^+$. The subsequent formation of $[MoH(C_2H_4)_2(dppe)_2]^+$ occurs by the two pathways defined by the rate equation (2) and illustrated in Fig. 2: the direct protonation of the equilibrium concentration of the parent complex [$k_1 = (4.60 \pm 0.1) \times 10^2$ (X = Cl), $(1.0 \pm 0.1) \times 10^5$ dm^3 mol^{-1} s^{-1} (X = Br)], and the intramolecular migration of a β-hydrogen atom from the ethyl ligand in $[Mo(C_2H_5)(C_2H_4)(dppe)_2]^+$ to the metal [$(k_3 + k_{-3}) = 0.22 \pm 0.01$ s^{-1} (X = Cl)]. It is to be expected that the rate for the intramolecular pathway is independent of the nature of the acid. Unfortunately the reaction with HBr, at phase (*ii*), is too rapid to allow a determination of $(k_3 + k_{-3})$, but the value of this parameter in the reactions with HBr can be determined at phase (*iii*) (see below). This interpretation of the initial reactions of *trans*-$[Mo(C_2H_4)_2(dppe)_2]$ with HX is identical to that for the analogous tungsten system,[2] with one minor difference. In the molybdenum case previous NMR spectroscopic studies [1] have shown that $[MoH(C_2H_4)_2(dppe)_2]^+$ and $[Mo(C_2H_5)(C_2H_4)(dppe)_2]^+$ are in rapid equilibrium and hence the rate constant determined for the intramolecular pathway is in reality the rate constant for the attainment of the equilibrium mixture, $(k_3 + k_{-3})$.

The direct protonation of the metal (k_1 pathway) is asso-

Table 3 Summary of the elementary rate constants and equilibrium constants for the reaction of *trans*-$[M(C_2H_4)_2(dppe)_2]$ (M = Mo or W) with HX (X = Cl or Br) in thf at 25.0 °C

M	Acid	K_x/dm^3 mol^{-1}	k_1/dm^3 mol^{-1} s^{-1}	K_2/dm^3 mol^{-1}	$(k_3 + k_{-3})$/s^{-1}	k_4/s^{-1}
W	HCl	4.1 ± 0.3	(2.0 ± 0.1) × 10^2 (k_H/k_D = 2.43)			
	HBr	(2.6 ± 0.2) × 10^2	(4.7 ± 0.4) × 10^4 (k_H/k_D = 1.0)			
Mo	HCl	18.0 ± 0.2	(4.6 ± 0.1) × 10^2 (k_H/k_D = 1.64)	*	0.22 ± 0.02	(3.1 ± 0.2) × 10^{-4}
	HBr	(7 ± 0.8) × 10^2	(1.0 ± 0.1) × 10^5	(1.77 ± 0.3) × 10^3	0.25 ± 0.02	

[a] k_2 = 14.0 ± 0.5 dm^3 mol^{-1} s^{-1}, $k_2 = K_2k_{-2}$.

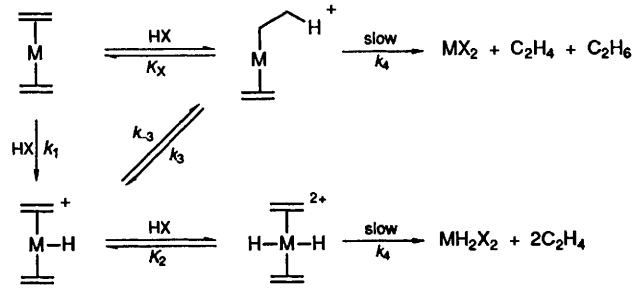

Scheme 3 Mechanism for the reaction of *trans*-$[Mo(C_2H_4)_2(dppe)_2]$ with HX (X = Cl or Br) in thf at 25.0 °C, showing the two pathways giving rise to ethane and ethylene. The phosphine ligands have been omitted for clarity, and the co-ordination environment shown for each molybdenum is a representation and has no implication for the true geometry of that species

ciated with a marked primary isotope effect, k_H/k_D = 1.64. The absence of a detectable isotope effect in the intramolecular migration pathway $(k_3 + k_{-3})$ as shown in Fig. 2 may, in part, be a consequence of the ground-state structure of the ethyl species. If this, formally sixteen-electron, species contains an agostic hydrogen, as shown in **1**, and proposed[7] for $[Mo(C_2H_5)(C_2H_4)(dppen)_2]^+$ (dppen = *cis*-$Ph_2PCHCHPPh_2$), then the migration to the metal requires only a minor movement of the hydrogen, with a corresponding small isotope effect.

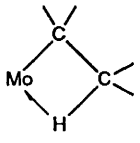

1

However, any discussion of the small isotope effect associated with a migration pathway following deuteriation of an ethylene ligand, as in this case, is complicated by the presence of the two hydrogen atoms bound to this carbon and their potential involvement rather than the deuterium in the migration step.[14]

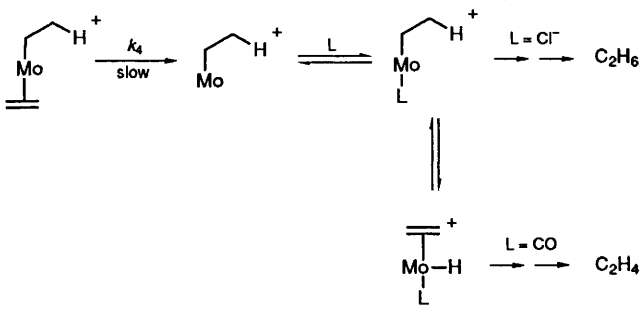

Scheme 4 Details of the post rate-limiting steps for the formation of ethane and ethylene in the reactions of *trans*-$[Mo(C_2H_4)_2(dppe)_2]$ with HX in thf at 25.0 °C, L = X^-, CO or H_2

The last phase [phase (*iii*)] observed on the stopped-flow time-scale corresponds to the further protonation of $[MoH(C_2H_4)_2(dppe)_2]^+$ to give $[MoH_2(C_2H_4)_2(dppe)_2]^{2+}$. Using HBr the kinetics of this phase [equation (3)] is consistent with a rapid protonation of $[MoH(C_2H_4)_2(dppe)_2]^+$ which perturbs the equilibrium of this species with $[Mo(C_2H_5)(C_2H_4)(dppe)_2]^+$ giving rise to the rate equation (4). This is consistent

$$k_{obs} = (k_3 + k_{-3})/(1 + K_2[HBr]) \quad (4)$$

with the experimental rate equation (3), and comparison of the two equations allows the calculation of K_2 = (1.77 ± 0.3) × 10^3 dm^3 mol^{-1} and $(k_3 + k_{-3})$ = 0.25 ± 0.01 s^{-1}. This value of $(k_3 + k_{-3})$ derived from the studies with HBr is in excellent agreement with that calculated earlier from the studies with HCl, and corroborates the proposal that the rate of this migration is independent of the nature of the acid.

The kinetics of phase (*iii*) with HCl is shown in Fig. 4 and is consistent with the same process as described for the HBr studies, namely protonation of $[MoH(C_2H_4)_2(dppe)_2]^+$ to give $[MoH_2(C_2H_4)_2(dppe)_2]^{2+}$ perturbing the equilibrium between the former species and $[Mo(C_2H_5)(C_2H_4)(dppe)_2]^+$. However, in the aprotic solvent thf, HCl is a weaker acid than HBr[15] resulting in slow protonation of $[MoH(C_2H_4)_2(dppe)_2]^+$ with HCl and changing the form of the rate equation to (2) with $a = (k_3 + k_{-3})$ = 0.22 ± 0.02 s^{-1} and $b = k_2$ = 14.0 ± 0.5 dm^3 mol^{-1} s^{-1} ($K_2 = k_2/k_{-2}$). Again the value of $(k_3 + k_{-3})$ is in excellent agreement with those determined earlier. The internal consistency of this value derived from different phases of the reaction, and in reactions with either acid, is good evidence that the mechanism we propose is correct.

Thus, at the end of phase (*iii*) in the reaction of *trans*-$[Mo(C_2H_4)_2(dppe)_2]$ with HX the reaction mixture consists primarily of three species: $[MoH(C_2H_4)_2(dppe)_2]^+$, $[MoH_2(C_2H_4)_2(dppe)_2]^{2+}$ and $[Mo(C_2H_5)(C_2H_4)(dppe)_2]^+$. The relative proportions of each are defined by the values of $(k_3 + k_{-3})$ and K_2, and this is reflected in the variation of the final absorbance with the acid concentration ([HCl] = 1 mmol dm^{-3}, A = 0.33; [HCl] = 50 mmol dm^{-3}, A = 0.16; [Mo] = 0.1 mmol dm^{-3}).

The Release of the Hydrocarbons.—The precursor complexes formed in the rapid protonation reactions of *trans*-$[Mo(C_2H_4)_2(dppe)_2]$ relatively slowly ($t_{\frac{1}{2}}$ *ca.* 40 min) release ethane and ethylene. The kinetics for the production of the gases is independent of (*a*) the concentration of HCl, (*b*) the hydrocarbon being formed and, (*c*) the presence of other gases such as carbon monoxide, as illustrated by the data in Tables 1 and 3. These observations suggest that the rate-limiting step for the formation of both gases is the dissociation of an ethylene ligand, k_4 = (3.1 ± 0.2) × 10^{-4} s^{-1}. Subsequent binding of halide ion or any other molecule present then facilitates the release of the remaining hydrocarbon as detailed in Scheme 4. This pathway is analogous to the mechanism established for protonation of

Table 4 Rate constants for protonation of the metal in *trans*-$[ML_2(dppe)_2]$ (M = Mo or W; L = N_2, C_2H_4 or 2 H) with HCl in thf at 25.0 °C

M	L	k/dm^3 mol^{-1} s^{-1}	k_{Mo}/k_W
Mo	N_2[a]	2.1×10^{-2}	7.8
W		2.7×10^{-3}	
Mo	H_2	$>1 \times 10^{6}$[b]	>172
W		5.8×10^{3}	
Mo	C_2H_4	4.6×10^{2}	2.3
W		2.0×10^{2}	

[a] First-order rate constants (s^{-1}), protonation from within outer-sphere adduct. [b] Not rate-limiting step.

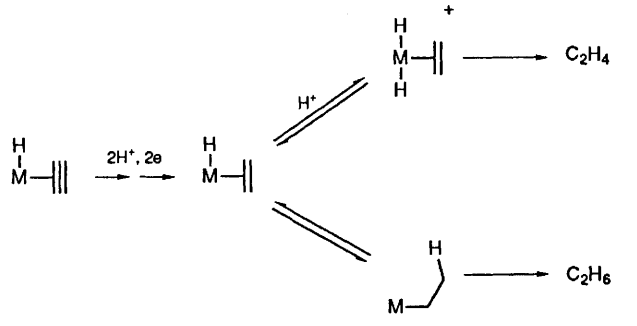

Scheme 5 Summary of the ethane-forming and ethylene-evolving pathways

trans-$[M(N_2)_2(dppe)_2]$ (M = Mo or W), where one dinitrogen ligand is protonated and the other is lost as dinitrogen gas.[16]

It is not possible to define which precursor complex(es) releases the hydrocarbons, or whether both ethane and ehtylene are released from the same species based on the kinetic data alone. The variation in the hydrocarbon product distribution with the concentration of HCl under an atmosphere of dinitrogen or argon shown in Fig. 5 allows us to define the species which give ethane and ethylene unambiguously. The data in Fig. 5 can be simulated as shown by the curve. This analysis uses the values of $(k_3 + k_{-3}) = 0.22$ s^{-1} and $k_2 = 14.0$ dm^3 mol^{-1} s^{-1}, derived from the kinetic analysis, to calculate the relative proportions of $[Mo(C_2H_5)(C_2H_4)(dppe)_2]^+$ and $[MoH_2(C_2H_4)_2(dppe)_2]^{2+}$. In addition *the data can be successfully simulated only if* $[Mo(C_2H_5)(C_2H_4)(dppe)_2]^+$ *produces* 1 *mole equivalent of both ethane and ethylene, whereas* $[MoH_2(C_2H_4)_2(dppe)_2]^{2+}$ *gives* 2 *mole equivalents of ethylene.* The success of this analysis using only the values of $(k_3 + k_{-3})$ and k_2 is because the rate-limiting step for the formation of the hydrocarbons $[k_4 = (3.1 \pm 0.2) \times 10^{-4}$ s$^{-1}]$ must be essentially the same for both $[Mo(C_2H_5)(C_2H_4)(dppe)_2]^+$ and $[MoH_2(C_2H_4)_2(dppe)_2]^{2+}$. This conclusion is certainly borne out by the invariance of k_4 over an acid concentration range where the relative proportions of the two precursor complexes changes.

Under an atmosphere of carbon monoxide the only gaseous product is ethylene, but this is not a consequence of carbon monoxide binding before the k_4 step since all the rate constants and equilibrium constants determined for the reaction of *trans*-$[Mo(C_2H_4)_2(dppe)_2]$ with HCl are unchanged whether measured under an atmosphere of dinitrogen, argon or carbon monoxide. Clearly carbon monoxide is binding to molybdenum after the rate-limiting k_4 step as illustrated in Scheme 4, and this binding affects the hydrocarbon product distribution by influencing the position of the equilibrium between the ethyl and ethylene, hydride species. With the electron-withdrawing carbon monoxide ligand the equilibrium position would appear to lie towards the hydrido-species, and facilitate the release of ethylene.

Under an atmosphere of dihydrogen the situation is more complicated, and it seems that binding of dihydrogen on the pathway originating from $[MoH_2(C_2H_4)_2(dppe)_2]^{2+}$ generates a species sufficiently 'hydride rich' that this pathway can now yield some ethane.

Protonation of the 'M(dppe)$_2$' *Core.*—The rate constants for the protonation of the metal in *trans*-$[ML_2(dppe)_2]$ (M = Mo or W; L = N_2, C_2H_4 or 2 H) by HCl are summarised in Table 4.[2,16–18] Irrespective of the nature of L the molybdenum centre is protonated faster than its tungsten analogue. This is a little surprising. Simple arguments based on relative bond strengths, size of the metal, steric forces or greater propensity of the heavier metal to attain a higher formal oxidation state suggest that protonation at tungsten would be faster. Relatively little is known about the factors influencing the rates of protonation of metal centres,[19] and this is the first time such a series has been investigated. We propose that two factors are important. First, the reorganisational energy of the 'ML$_2$(dppe)$_2$' core upon binding a proton, and secondly the electron density at the metal. Either would appear to dominate the reactivity in these systems.

The greater ease of protonation of the molybdenum site compared to its tungsten counterpart is also reflected in diprotonation of the species $[MoH_4(dppe)_2]$[17] and $[Mo(C_2H_4)_2(dppe)_2]$, but only monoprotonation in tungsten analogues.[2,18]

Factors influencing the Formation of Ethane and Ethylene: Relevance to the Action of Nitrogenases.—The factors which discriminate between ethane formation and ethylene evolution are summarised in Scheme 5. The study we have described offers a rationale of the substrate specificity shown by the molybdenum- and vanadium-based nitrogenases,[3,4] in which acetylene is reduced to ethane only by the latter. All else being the same, it may be that the vanadium-based active site (a Group 5, first-row transition metal) would be less basic and less electron-releasing than an analogous molybdenum-centre (a Group 6, second-row transition metal). Thus the molybdenum-based enzyme may be more susceptible to protonation resulting in the evolution of ethylene, whereas the vanadium site has a greater opportunity to proceed unhindered through the pathway to yield ethane. Of course this study tells us nothing about the mechanism of the initial stages of the reduction of acetylene to ethylene.

Experimental

All manipulations in the preparative and mechanistic aspects of this work were routinely performed under an atmosphere of dinitrogen or argon using standard Schlenk or syringe techniques as appropriate. All IR spectra were recorded on a Perkin-Elmer 883 spectrometer in Nujol mulls, NMR spectra on a JEOL GSX 270 spectrometer and UV/VIS spectra on a Perkin-Elmer Lambda 5 spectrophotometer. Gas samples were analysed on a Philips PU 4400 gas–liquid chromatograph and computing integrator PU 4815 equipped with a Poropak Q column at 130 °C. The identity of the gases detected was established by comparison of the retention times with those of authentic samples of the gases.

Kinetic Studies.—(*i*) *Stopped-flow studies.* All solutions were prepared under an atmosphere of the required gas, and transferred by gas-tight syringe into the stopped-flow apparatus. Solutions of anhydrous HX were prepared from stock solutions, which in turn were prepared from equimolar amounts of $SiMe_3X$ and MeOH (or MeO^2H, when requiring deuterioacids). All solutions were used within 1 h of preparation.

A Hi-Tech Scientific SF-51 stopped-flow spectrophotometer was used, modified to handle air-sensitive solutions. The temperature was maintained at 25.0 °C using a Grant LE8 thermostat connected to the spectrophotometer. The stopped-flow apparatus was interfaced to a B.B.C. microcomputer (Acorn Computers, Cambridge) *via* an analogue-to-digital

converter operating at 3 kHz. The data were stored on a $5\frac{1}{4}$ in (*ca.* 0.13 m) diskette, and analysed by standard curve-fitting procedures. Analysis of the results was by the necessary straight-line graphs and errors were established by a linear least-squares analysis.

(*ii*) *Gas evolution.* In a typical gas-analysis experiment, a round-bottomed, two-necked flask (500 cm^3) was used. One neck was fitted with a gas-tight tap and the other with a rubber septum. In an atmosphere of the required gas (argon, di-nitrogen, carbon monoxide or dihydrogen) the flask was charged with a solution of *trans*-$[Mo(C_2H_4)_2(dppe)_2]$ (1×10^{-4} mol dm^{-3}) in thf (25 cm^3). The flask was then sealed by closing the gas-tight tap, placed in a Grant SE10 thermostatted tank at 25.0 °C and a solution of anhydrous HCl added such that the final concentration of acid in the flask was known. For kinetic studies, samples (0.1 cm^3) of gas were taken at various times for *ca.* 3 h and analysed by GLC. The concentration of each gas in the sample was calculated by prior calibration of the Poropak Q column with a known concentration of the gases. The kinetic data were analysed by the normal semilogarithmic graph,[20] and the plots were linear for at least three half-lives. For product analysis, the gases were sampled after *ca.* 5 h.

Preparations.—trans-*Bis*[1,2-*bis*(*diphenylphosphino*)*ethane*]-*bis*(*ethylene*)*molybdenum.* This complex was prepared by the method outlined in the literature.[1] Ethylene was bubbled through a suspension of *trans*-$[Mo(N_2)_2(dppe)_2]$[21] in thf for *ca.* 2 h and then the flask was stoppered under an atmosphere of ethylene and stirred vigorously for 18 h. At the end of this period the solvent was removed *in vacuo* until incipient precipitation of the product. A large excess of methanol was added to complete the precipitation of essentially pure material. Subsequent recrystallisation from thf–methanol gave pure product. Yield = 80%.

Bis[1,2-*bis*(*diphenylphosphino*)*ethane*]*ethylenedihydrido-molybdenum dibromohydrogenate.* To a solution of *trans*-$[Mo(C_2H_4)_2(dppe)_2]$ (0.10 g, 0.11 mmol) in thf (20 cm^3) was added (without stirring) a solution of anhydrous HBr (5 cm^3, 0.1 mol dm^{-3} in thf). Within a few minutes orange crystals were deposited, removed by filtration, washed with diethyl ether and dried *in vacuo.* Yield = 0.07 g (60%).

References

1 J. W. Byrne, H. U. Blaser and J. A. Osborne, *J. Am. Chem. Soc.*, 1975, **97**, 3871.
2 R. A. Henderson and K. E. Oglieve, *J. Chem. Soc., Chem. Commun.*, 1991, 584.
3 M. J. Dilworth, *Biochim. Biophys. Acta*, 1966, **127**, 285.
4 M. J. Dilworth, R. R. Eady, R. L. Robson and R. W. Miller, *Nature (London)*, 1987, **327**, 167.
5 G. A. Ashby, M. J. Dilworth and R. N. F. Thorneley, *Biochem. J.*, 1987, **247**, 547.
6 J. W. Byrne, J. R. M. Kress, J. A. Osborne, L. Ricard and R. E. Weiss, *J. Chem. Soc., Chem. Commun.*, 1977, 662.
7 M. L. H. Green and L.-L. Wong, *J. Chem. Soc., Chem. Commun.*, 1988, 677.
8 J. Halpern, L. Cai, P. J. Desrosiers and Z. Lin, *J. Chem. Soc., Dalton Trans.*, 1991, 717.
9 J. Chatt, G. A. Heath and R. L. Richards, *J. Chem. Soc., Dalton Trans.*, 1974, 2074.
10 R. H. Crabtree, G. G. Hlatky, C. P. Parnell, B. E. Segmuller and R. J. Uriarte, *Inorg. Chem.*, 1984, **23**, 354 and refs. therein.
11 R. Ellis, R. A. Henderson, A. Hills and D. L. Hughes, *J. Organomet. Chem.*, 1987, **333**, C6.
12 R. A. Henderson, D. L. Hughes, R. L. Richards and C. Shortman, *J. Chem. Soc., Dalton Trans.*, 1987, 1115.
13 J. D. Lane and R. A. Henderson, *J. Chem. Soc., Dalton Trans.*, 1987, 197 and refs. therein.
14 J. K. Kochi, *Organometallic Mechanisms and Catalysis*, Academic Press, New York, 1978, ch. 12 and refs. therein.
15 R. P. Bell, *The Proton in Chemistry*, 2nd edn., Chapman and Hall, London, 1973, ch. 4.
16 R. A. Henderson, *J. Chem. Soc., Dalton Trans.*, 1982, 917.
17 R. A. Henderson, *J. Chem. Soc., Chem. Commun.*, 1987, 1670.
18 R. A. Henderson, unpublished work.
19 R. T. Edidin, J. M. Sullivan and J. R. Norton, *J. Am. Chem. Soc.*, 1987, **109**, 3945 and refs. therein.
20 J. H. Espenson, *Chemical Kinetics and Reaction Mechanism*, McGraw-Hill, New York, 1981, ch. 2, p. 12.
21 J. R. Dilworth and R. L. Richards, *Inorg. Synth.*, 1980, **20**, 126.

Received 20*th June* 1991; *Paper* 1/03051E